QSM4SENIOR: Quantitative susceptibility mapping in the aging of the healthy brain.

Miguel Guevara[1,2], Davy Cam[3], Jacques Badagbon[3], Michel Bottlaender[2], Yann Cointepas[1,2], Jean-François Mangin[1,2], Ludovic de Rochefort[3] and Alexandre Vignaud[1,2]

[1] CNRS BAOBAB UMR9027 Gif-Sur-Yvette, France; [2] CEA NeuroSpin, Gif-Sur-Yvette; [3] VENTIO, Marseille, France

Introduction: The population of developed countries is aging, which is associated with an increase of neurodegenerative diseases. Several studies aim at documenting this phenomenon. One of them, The SENIOR study, consists in an annual follow-up examinations over 10 years of elderly healthy volunteers with several biomarkers (genetic, biological, imaging) [1]. It includes high-field 7T magnetic resonance imaging (MRI[ab]) acquisitions for high-resolution brain characterization.

There is an increasing evidence that iron accumulates in the aging brain, therefore its quantification could be used as a biomarker for the evaluation of the normal brain aging as well as to measure the severity of certain pathologies [2][3]. Quantitative susceptibility mapping (QSM) provides a quantitative metric linked to iron load in specific regions of interest [4], and increased QSM values for the regions implicated with the neuropathologies have been reported [2]. The accumulation of iron at different ages has been mostly analyzed by cross-sectional studies, which do not allow to address it at individual level over time. Moreover, these studies have been mostly performed at 3T. Ultra-high magnetic fields can provide a greater sensibility and a higher resolution [5]. However these acquisitions can also be more vulnerable to artifacts or effects from strong field variations due to air/tissue interface that need to be filtered out [3].

The QSM4SENIOR project, supported by the EOSC-Life[c] industry-academia collaboration call and presented in this work, aims at studying the accumulation of iron by using QSM in the SENIOR database. We implemented a phase pre-processing pipeline to reduce the presence of artifacts in the 7T MRI data, due to their higher inhomogeneities sensitivity to strong background field or arising from improper coil combination for the phase reconstruction (or both). The resulting filtered field was used it as input for the MEDI algorithm [6]. Moreover, the pipeline was deployed in the infrastructure provided by de.NBI Cloud[d], providing an ISO27001-certified Openstack cloud infrastructure. Here, we show these preliminary steps. QSM data will then be correlated with age as well as with other biomarkers available in SENIOR, and the curated data will be FAIRified and made available for research.

Methods: (I) Participants: 84 volunteers (50 -70 years old at the time of inclusion, 41 males/43 females, 78 right-handed and 6 left-handed) were selected from the SENIOR database [1]. 41 subjects present 1 visit at the time this study was conducted and 43 with 2 visits.

(II) Image acquisition: The MRI data was acquired at NeuroSpin (Gif-sur-Yvette, France) on a 7Tesla MRI system (Magnetom 7 Tesla scanner, Siemens Healthineers, Erlangen, Germany) 1Tx/32Rx Nova Medical head coil. Multi-gradient-echo acquisition (MGRE) was performed for QSM (TA=9:48 min, FoV=256 mm, voxel size=0.8 mm isotropic, TR=37 ms, TE=1.68 ms, ΔTE=3.05 ms, number of echoes=10, flip angle=30°, acceleration factor GRAPPA=3, 196 sagittal partitions, bandwidth=740 Hz/px, monopolar readouts) as well as B_1^+ and B_0 maps for calibration and correction purposes. The T1-weighted MP2RAGE was also acquired (TR= 6000 ms; TE=2.96 ms; voxel size=0.75 mm isotropic). MGRE data was reconstructed using Virtual Coil Combination (VCC) [7].

(III) Cloud computing: Computing resources (14 cores - 32 Go RAM virtual machines with 200 Go volumes) were deployed and configured automatically to create a secure instance running the pipeline in the de.NBI cloud. Imaging data were encrypted on transit and at rest.

(IV) Data processing: The method consists in pre-filtering the phase data from the MGRE acquisition by using the information of the magnitude and phase from the ten available echoes. It is based on the method described in [8], where in order to isolate the brain internal field variations (ΔB_{in}) the conjugate gradients algorithm of the normal equation $\Delta W_\Delta^2 \Delta B_{in} = \Delta W_\Delta^2 \Delta B$ is calculated, where W_Δ is a diagonal matrix weighting each estimation of the Laplacian by the inverse of its error standard deviation. The unwrapping is included in the analysis by forcing the point by point difference between]-π, π] when calculating ΔB using the modulo function. The processing starts with the calculation of the Laplacian of the field. In order to do that, the Laplacian of the phase for each echo k is computed (ΔB_k), as well as its error ($W_{\Delta k}$), before being combined in the least-squares sense. The gradient norm of the field was also computed similarly.

[a] Neurospin 7T received funding from the France-Life-Imaging project – grant 11-INBS-0006

[b] This work has been supported by the Leducq Foundation large equipment ERPT program, the NEUROVASC7T project, the Institut Carnot.

[c] This project has received funding from the European Union's Horizon 2020 research and innovation programme under grant agreement No 824087 – European Open Science Cloud in Life Sciences.

[d] This work was supported by the BMBF-funded de.NBI Cloud within the German Network for Bioinformatics Infrastructure (de.NBI) (031A532B, 031A533A, 031A533B, 031A534A, 031A535A, 031A537A, 031A537B, 031A537C, 031A537D, 031A538A).

A mask containing only the voxels with reliable information was then computed. It stems from a whole-brain mask refined using the information from the gradient of the field. The whole-brain mask is computed using Advanced Normalization Tools (ANTs) from the T1-weighted. The T1 is registered by a rigid transformation to the magnitude of the MGRE first echo, for applying this transformation to the mask. The gradient norm of the field is used to remove voxels suffering from spatial deformation (such as the region near the sinus) leading to a ΔB_{in} that cannot be correctly measured. A first restriction of the analysis to the area inside the brain is performed given by the whole-brain mask. Then a thresholding step keeps only the reliable voxels. Morphological operations in order to eliminate isolated voxels and filling of holes (opening, connected components algorithm and closing) are then done. Finally, an erosion is included in order to remove voxels from the brain periphery. At last, the conjugate gradient algorithm is used to compute B_{in} from the normal equation. Iterations were stopped when number of maximum iterations is reached (512) or the relative norm was less than 10^{-3}.

Results and Discussions: Figure 1 shows an example of a cloud-computed QSM from the reconstructed unwrapped filtered phase and the customized mask (D). The default results from the unprocessed T2* data (A) are also displayed. It can be seen that the refinement of the brain mask (B) allows to remove from the QSM computation some unreliable input voxel values. Moreover, the computation of filtered phase map from all the available echoes helps overcoming the presence of artifacts such as open-ended fringe lines arising from a poor coil combination. This allowed us to give a cleaner input into the MEDI algorithm (C), obtaining QSM with reduced artifacts (D). This preliminary result indicates that the pre-processing pipeline may be used in the presence of phase error resulting from improper coil combination with open-ended fringe lines. Furthermore, the implementation of the pipeline in a virtual infrastructure demonstrates the capacity of remote processing of research data in secure environments with adequate security measures. Indeed, this offers the possibility of analyzing the whole cohort importing into the servers the DICOM raw data, run the pipeline and then export the results back, with optimized cloud computing resource scheduling.

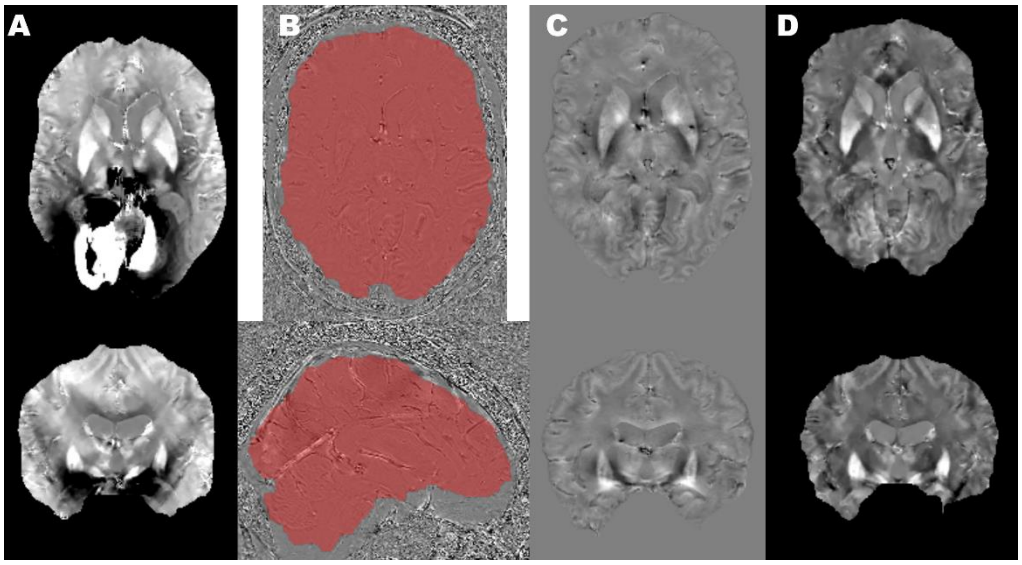

Figure 1 – QSM obtained using projection-onto-dipole field (PDF [9]) (A); Laplacian of the phase with the filtered mask overlayed (B); Result of the filtered field map (rdf), from the conjugate gradients calculation (C); QSM obtained with the internal field (D).

Conclusions: In this work we presented preliminary brain QSM results of the SENIOR database, as a proof of concept, for the cloud-based reconstruction. We developed a field pre-processing pipeline aiming at reducing the presence of artifacts in the input phase data in order to compute cleaner QSM maps. Although the results are preliminary and the method is still to be refined, it is promising because it allowed us to retrieve the information from the available data. Moreover, the automatic nature of the pipeline will allow us to apply it to a cohort in order to perform posterior statistic analyses. The incorporation of QSM data to the SENIOR database will add the quantification of iron as a valuable biomarker in the normal aging of the brain.

References:

[1] Haeger, A., et al. (2020). Imaging the aging brain: study design and baseline findings of the SENIOR cohort. *Alzheimer's research & therapy*, vol. 12(1), article 77, https://doi.org/10.1186/s13195-020-00642-1 .
[2] Ravanfar, P., et al. (2021). Systematic review: quantitative susceptibility mapping (QSM) of brain iron profile in neurodegenerative diseases. *Frontiers in neuroscience*, 41.
[3] Wang, C., et al. (2022). Phenotypic and genetic associations of quantitative magnetic susceptibility in UK Biobank brain imaging. *Nature Neuroscience*, 1-14.
[4] Ruetten, P., et al. (2019). Introduction to quantitative susceptibility mapping and susceptibility weighted imaging. *The British Journal of Radiology*, 92(1101), 20181016.
[5] Wang, Y., et al. (2009, September). Magnetic source MRI: a new quantitative imaging of magnetic biomarkers. In *2009 Annual International Conference of the IEEE Engineering in Medicine and Biology Society* (pp. 53-56). IEEE.
[6] Liu, T., et al. (2011). Morphology enabled dipole inversion (MEDI) from a single-angle acquisition: comparison with COSMOS in human brain imaging. *Magnetic resonance in medicine*, 66(3), 777-783.
[7] Blaimer, M., et al. (2016). Comparison of phase-constrained parallel MRI approaches: Analogies and differences. *Magnetic resonance in medicine*, 75(3), 1086-1099.
[8] de Rochefort, L., et al. (2009). Quantitative susceptibility mapping in vivo in the rat brain. *Proc Intl Soc Magnet Reson Med*, 17(c), 1134.
[9] Liu, T., et al. (2011). A novel background field removal method for MRI using projection onto dipole fields. *NMR in Biomedicine*, 24(9), 1129-1136.